Clinical Cancer Research

An Anti–CLL-1 Antibody–Drug Conjugate for the Treatment of Acute Myeloid Leukemia

Bing Zheng, Shang-Fan Yu, Geoffrey del Rosario, Steven R. Leong, Genee Y. Lee, Rajesh Vij, Cecilia Chiu, Wei-Ching Liang, Yan Wu, Cecile Chalouni, Jack Sadowsky, Vanessa Clark, Angela Hendricks, Kirsten Achilles Poon, Wayne Chu, Thomas Pillow, Melissa M. Schutten, John Flygare, and Andrew G. Polson

Abstract

Purpose: The treatment of acute myeloid leukemia (AML) has not significantly changed in 40 years. Cytarabine- and anthracycline-based chemotherapy induction regimens (7 + 3) remain the standard of care, and most patients have poor long-term survival. The reapproval of Mylotarg, an anti-CD33–calicheamicin antibody–drug conjugate (ADC), has demonstrated ADCs as a clinically validated option to enhance the effectiveness of induction therapy. We are interested in developing a next-generation ADC for AML to improve upon the initial success of Mylotarg.

Experimental Design: The expression pattern of CLL-1 and its hematopoietic potential were investigated. A novel anti–CLL-1-ADC, with a highly potent pyrrolobenzodiazepine (PBD) dimer conjugated through a self-immolative disulfide linker, was developed. The efficacy and safety profiles of this ADC were evaluated in mouse xenograft models and in cynomolgus monkeys.

Results: We demonstrate that CLL-1 shares similar prevalence and trafficking properties that make CD33 an excellent ADC target for AML, but lacks expression on hematopoietic stem cells that hampers current CD33-targeted ADCs. Our anti–CLL-1-ADC is highly effective at depleting tumor cells in AML xenograft models and lacks target independent toxicities at doses that depleted target monocytes and neutrophils in cynomolgus monkeys.

Conclusions: Collectively, our data suggest that an anti–CLL-1-ADC has the potential to become an effective and safer treatment for AML in humans, by reducing and allowing for faster recovery from initial cytopenias than the current generation of ADCs for AML.

Introduction

The treatment of acute myeloid leukemia (AML) has not significantly changed in 40 years, and most patients have poor long-term survival. Cytarabine- and anthracycline-based chemotherapy induction regimens (7 + 3) remain the standard of care (SOC) for newly diagnosed <60-year-old patients with AML and a subset of >60-year-old medically fit patients. This regimen achieves complete remission (CR) ranging from 50% to 80% (1, 2). Unfortunately, 60% to 70% of patients under the age of 60 years who achieve a CR will relapse, highlighting the need for more effective therapies to achieve more durable remissions. Advancement of targeted therapies provides new hopes and options to subsets of patients with AML carrying specific mutations with two approvals in 2017 by the FDA. Rydapt (midostaurin, Novartis) in combination with SOC chemotherapy improved 4-year overall survival (OS) from 44.3% to 51.4% for patients with fms-related tyrosine kinase 3 (FLT3) mutation (3); Idhifa (enasidenib, Celgene) increased the median OS to 9.3 months for relapsed and refractory patients with an isocitrate dehydrogenase-2 (IDH2) mutation (4). However, additional therapeutics are needed to improve outcomes for the remaining of majority patients with AML.

Recently, several lines of evidence suggest that patient outcomes can be improved if the intensity of induction chemotherapy can be safely increased. In combination with cytarabine, high-dose daunorubicin (90 mg/m^2) compared with a standard dose (45 mg/m^2) resulted in a higher rate of CR and improved OS (5). Utilizing a unique liposomal formulation to increase the uptake and exposure of daunorubicin and cytarabine, Vyxeos (CPX-351, Jazz Pharmaceuticals) has been recently approved by the FDA based on OS advantage over the SOC (6). Another way to enhance the effectiveness of induction chemotherapy is to use an ADC to deliver a more potent cytotoxic payload specifically targeting leukemia cells while maintaining lower systemic concentrations. The reapproval of Mylotarg (gemtuzumab ozogamicin, Pfizer), an anti-CD33–calicheamicin ADC, has demonstrated ADCs as a clinically validated option in treatment of AML. Nevertheless, more recent developments in ADC technology such as stable linker designs and site-directed conjugation have the potential to improve on the initial success of gemtuzumab ozogamicin.

Research and Early Development, Genentech Inc., South San Francisco, California.

Note: Supplementary data for this article are available at Clinical Cancer Research Online (http://clincancerres.aacrjournals.org/).

B. Zheng and S.-F. Yu contributed equally to this article.

Current address for A. Hendricks: Denali Therapeutics, South San Francisco, CA; current address for K.A. Poon, Amgen, South San Francisco, CA; and current address for J. Flygare, Merck, South San Francisco, CA.

Corresponding Authors: Andrew G. Polson, Genentech, Inc., 1 DNA Way, South San Francisco, CA 94080. Phone: 650-225-5134; Fax: 650-225-6240; E-mail: polson@gene.com, and Bing Zheng, Phone: 650-225-2964; E-mail: zheng.bing@gene.com

doi: 10.1158/1078-0432.CCR-18-0333

Translational Relevance

The reapproval of Mylotarg has demonstrated antibody–drug conjugates (ADC) as a clinically validated option to enhance the effectiveness of induction therapy for acute myeloid leukemia (AML) by delivering a more potent cytotoxic payload specifically targeting leukemia cells while maintaining lower systemic concentrations. Here, we describe the development of a novel anti–CLL-1-ADC, with a highly potent PBD dimer conjugated through a self-immolative disulfide linker. Our preclinical data demonstrate that anti–CLL-1-ADC is highly effective at depleting tumor cells in AML xenograft models and lacks target independent toxicities at doses that depleted target myeloid cell in cynomolgus monkeys. We also provide evidence that a therapy targeting CLL-1 probably will have less impact on normal hematopoiesis than targeting CD33 and may provide better hematopoietic recovery for treated patients. These findings support the potential clinical benefits of anti–CLL-1-ADC as an effective and safer treatment for AML in humans, and its better combinability with other therapeutics.

Although the clinical benefit of gemtuzumab ozogamicin has been demonstrated, a number of potential limitations to an even greater clinical benefit have been identified. CD33 is expressed on $CD34^+/CD38^-$ hematopoietic stem cells (HSC; refs. 7–9) and, unlike the commonly used microtubule inhibitors, DNA-damaging agents can be effective against noncycling cells. Consequently, a potent CD33-targeting ADC with a DNA-damaging agent could delay or eliminate bone marrow recovery in patients with AML, consistent with what is observed with vadastuximab talirine (SGN-CD33A, Seattle Genetics; ref. 10). An attractive alternative target for an AML ADC is the C-type lectin-like molecule-1 (CLL-1). CLL-1, also known as C-type lectin domain family 12 member A (CLEC12A), is only presented on the surface of committed myeloid cells but is absent on normal HSCs (9, 11–14). This suggests that although a CLL-1 ADC will still be expected to cause initial myelosuppression, it has the potential to spare platelets, lymphocytes, and speed up the recovery of myeloid cells compared with CD33-targeted ADCs. Furthermore, it has been shown to be overexpressed in nearly all AMLs and is implicated as a marker of leukemia stem cells (LSC; refs. 11, 12, 15–17). Therefore, an anti–CLL-1 ADC containing a highly potent pyrrolobenzodiazepine (PBD) dimer DNA alkylating and cross-linking agent, conjugated through a novel self-immolative disulfide linker, could be an effective and safer treatment for AML.

Materials and Methods

Target expression by flow cytometry

AML cell lines, human blood, and bone marrow (from healthy donors and patients with AML) were stained as described previously (9) using the following antibody reagents: anti-human CLL-1-PE antibody (R&D Systems), anti-human CD10-BV605 antibody, anti-human CD34-APC antibody, anti-human CD38-APC-R700 antibody, anti-human CD45RA-PE-Cy7 antibody, anti-human CD135-BV421 antibody and 7-amino-actinomycin D (7-AAD; BD Biosciences). Samples were acquired on LSRII flow cytometer (BD Biosciences). Data were analyzed using FlowJo.

Bone marrow or peripheral blood mononuclear cells (PBMC) were isolated by Ficoll density gradient centrifugation from remnant patient samples with confirmed AML disease. The measurement of CLL-1 and CD33 expression on AML blasts were performed using an AML-specific quantitative FACS assay (Genoptix) with PE-conjugated anti-CD33 and anti–CLL-1 antibodies (Genentech). AML blasts were identified by labeled anti-CD markers (CD13, CD34, CD117, HLA-DR, and CD33; BD Biosciences). All samples were run in the presence of Quantibrite beads for quantitation of the CD33 and CLL-1 signals. CLL-1 and CD33 expressions were normalized by their PE molecule/antibody ratio and displayed as number of antibodies bound.

Colony-forming cell assay

Bone marrow mononuclear cells (BM-MNC) from healthy human donors (AllCells) were prepared by density gradient centrifugation with Ficoll–Paque PLUS (GE Healthcare). $CD34^+$ cells were then isolated from the BM-MNCs using the Miltenyi Diamond CD34 Isolation Kit (Miltenyi Biotec) and cultured for 36 hours in StemSpan SFEM medium supplemented with recombinant human cytokines cocktail CC100 (Flt3L, SCF, IL3, and IL6) from STEMCELL Technologies before the cells were sorted by FACS into two separate populations of $CD34^+/CLL\text{-}1^+$ and $CD34^+/CLL\text{-}1^-$ cells. Colony-forming cell (CFC) assay using MethoCult Enriched medium (STEMCELL Technologies) was performed according to the manufacturer's protocol. After 10 days, colonies were counted and scored for multi-lineage [colony-forming unit-granulocyte/erythroid/macrophage/megakaryocyte (CFU-GEMM)], erythroid [burst-forming unit-erythrocyte or colony-forming unit – erythrocyte (B/CFU-E)], and myeloid morphology [colony-forming unit-granulocyte/macrophage (CFU-GM)].

Target internalization

Antibodies to CLL-1 and CD33 were labeled with DyLight 488 Antibody Labeling Kit (Thermo Fisher Scientific) according to the manufacturer's protocol. For lysosomal trafficking, cells were first incubated with 50 nmol/L of LysoTracker Red DND-99 (Thermo Fisher Scientific) for 2 hours under growth conditions to label the acidic compartments. Otherwise, cells were preblocked to reduce nonspecific binding to FcγRs with 1,000 μg/mL of human IgG in fresh media and transferred to Nunc Lab-Tek II Chamber Slide System (Thermo Fisher Scientific). DyLight-488–labeled anti–CLL-1 antibody was added to the wells at 10 μg/mL. Images were acquired at different time points using an HCX PL APO CS 63 × 1.40 oil immersion lens with a digital zoom of 2.5× on a Leica SP5 confocal microscope (Leica Microsystems) dotted with a Ludin environmental chamber.

Antibody and THIOMAB ADCs

Antibodies to CLL-1 were produced and humanized at Genentech using previously described methods (9). Antibody cross-reactivity to recombinant and endogenous cynomolgus monkey (cyno) CLL-1 was determined by FACS using 293 cells overexpressing recombinant cyno CLL-1 and cyno PBMCs, respectively.

PBD dimer was conjugated to the CLL-1 THIOMAB antibody through a disulfide bond between the linker thiol moiety and the

engineered cysteine thiol, according to previously described methods (18, 19).

Epitope mapping

The epitope of the CLL-1 antibody was characterized by hydroxyl radical footprinting (NeoProteomics). Briefly, the free antigen and antigen–antibody complex were exposed to hydroxyl radicals for intervals of 0, 10, 15, and 20 ms using the X28c Beam line at the Brookhaven National Laboratory. The labeled samples were subjected to liquid chromatography coupled with high-resolution mass spectrometry (LC-MS). The MS data were analyzed using ProtMapMS to generate dose–response plot and calculate the rate constant (RC) for each peptide. The solvent-protected regions in the complex experience diminished oxidation reaction as opposed to the free antigen. Protection ratio (PR) is defined as $RC_{antigen}/RC_{complex}$. Differences in the rate of oxidation serve to highlight the location of the epitope (20).

Cell viability assay

Cell viability assays were performed as described previously (21). AML primary patient samples were cultured in Iscove's Modified Dulbecco's Medium supplemented with 20% heat-inactivated human serum, recombinant human cytokines cocktail CC100, and 50 ng/mL each of G-CSF and GM-CSF (STEMCELL) for one day after thawing. Tumor cells were then blocked with excess amount of mouse IgG2a anti-ragweed antibody and treated with ADCs for 6 days at 37°C before cell viability was measured. The same assay conditions were also used for AML cell lines.

In vivo efficacy xenograft experiments

All animal studies were performed in compliance with NIH Guidelines for the Care and Use of Laboratory Animals and were approved by the Institutional Animal Care and Use Committee (IACUC) at Genentech, Inc.

Three human AML cell lines, EOL-1 (DSMZ), HL-60, and THP-1 (ATCC) were used to establish subcutaneous xenograft models for evaluation of anti–CLL-1-ds-PBD efficacy. Tumor cells (5×10^6 EOL-1 or HL-60, or 1×10^7 THP-1 cells suspended in 0.1 mL of Hanks' Balanced Salt Solution supplemented with Matrigel) were inoculated to the flank of female C.B-17 Fox Chase SCID mice (Charles River Laboratories). When mean tumor size reached the desired volume (~200 mm^3), animals were randomized into groups of $n = 8$, each with similar mean tumor size, and received an intraperitoneal dose of a mouse IgG2a anti-ragweed antibody in excess amount (30 mg/kg) to block FcγRs frequently expressed on the surface of AML cells. Four hours later, animals in each group were given a single intravenous dose of vehicle, anti–CLL-1 antibody or ADCs through the tail vein. Treatment groups were not blinded during tumor measurement. Tumors were measured in two dimensions (length and width) using calipers, and the tumor volume was calculated using the formula: tumor size (mm^3) = 0.5 × (length × width × width). The results were plotted as mean tumor volume ± SEM of each group over time.

To set up a disseminated AML xenograft model, HL-60 cells (2×10^7 cells suspended in 0.1 mL of HBSS) were given intravenously to female C.B-17 SCID mice through the tail vein. Bone marrow from selected animals was collected periodically to assess tumor burden. When tumor burden reached the desired level (~30%), animals were randomized into groups of $n = 5$ each and received an intraperitoneal dose of a mouse IgG2a anti-ragweed antibody in excess amount (30 mg/kg) to block FcγRs frequently expressed on the surface of AML cells. Four hours later, animals in each group were given a single intravenous dose of vehicle or ADCs. Mice were monitored until 2 weeks postdose when the vehicle group displayed adverse clinical symptoms (including >20% weight loss, hind leg paralysis, ruffled fur, and/or hunched posture), at which point all animals were euthanized. Bone marrow was collected from both femurs to evaluate treatment effects on tumor burden.

Leukocytes were isolated from mouse bone marrow via ammonium chloride lysis of erythrocytes. Cells were stained with FITC mouse anti-human HLA-ABC and 7-AAD (BD Biosciences). Samples were acquired by FACSCalibur (BD Biosciences) and data were analyzed by FlowJo software. HL-60 tumor cells were identified by surface expression of HLA, and tumor burden was quantitated as the percentage of HL-60 tumor cells relative to total viable leukocytes (i.e., 7-AAD^- cell population) isolated from mouse bone marrow. The results were plotted for individual animal and mean (±SEM) tumor burden of each treatment group.

Toxicity study in cynomolgus monkeys

All procedures in animals were performed in compliance with the Animal Welfare Act, the Guide for the Care and Use of Laboratory Animals, and the Office of Laboratory Animal Welfare. Protocols were reviewed and approved by the IACUCs of Charles River Laboratories. Cynomolgus monkeys were allocated into 5 groups (n = 2–3/sex/group). Animals were administered 0 (vehicle), 0.1, or 0.2 mg/kg anti–CLL-1-ds-PBD as a single intravenous dose on day 1 and were euthanized on day 25 or 26. Additional animals (n = 2/sex/group) were administered 0.4 or 1.0 mg/kg anti–gD-ds-PBD as two intravenous doses on days 1 and 22 and were euthanized on day 43. Toxicity parameters consisted of clinical observations, bodyweight measurements, food consumption, physical examinations, ophthalmic examinations, clinical pathology, organ weights, and histopathology. Necropsies included examination of the carcass, external body orifices, abdominal, thoracic, and cranial cavities, and organs. Tissues collected at necropsy were preserved in 10% neutral-buffered formalin or modified Davidson's fixative and were processed for routine histologic examination. Select organs were weighed prior to fixation.

Results

CLL-1 has similar copy number and prevalence in AML as CD33

First, we wanted to validate the expression of CLL-1 in patients with AML as a potential ADC target by comparing it with the well-validated and prevalent target, CD33. Seventy remnant AML patient samples were purified by Ficoll density gradient centrifugation, immunophenotyped by FACS (see Materials and Methods) and analyzed for surface expression of CLL-1 and CD33 on AML blasts. CLL-1 and CD33 expression levels were normalized by their PE molecule/antibody ratio and displayed as the number of antibodies bound (Fig. 1A). CLL-1 exhibited similar prevalence as CD33, with slightly lower median expression (1,525 vs. 1,863 antibodies

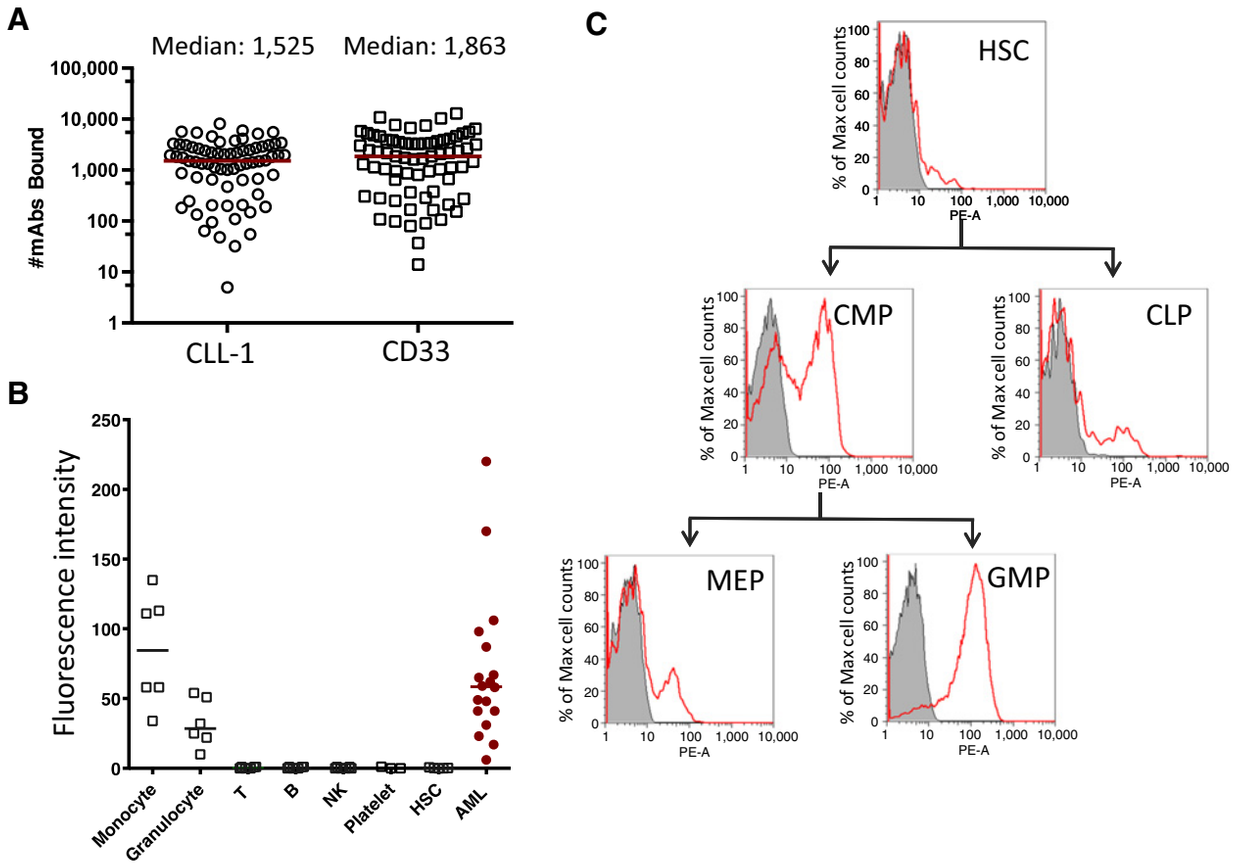

Figure 1.

CLL-1 expression in patients with AML and normal donors. **A,** Comparison of CLL-1 (open circle) and CD33 (open square) expression level in 70 patients with AML. Expression level was normalized to antibody bound by Quantibrite beads and PE molecule/antibody ratio. Solid line, median value of expression. **B,** CLL-1 expression in normal leukocytes (black open square) and patients with AML (cayenne solid circle). Solid line, median value of expression. **C,** Representative expression of CLL-1 in different stage of hematopoietic stem cell and progenitor cells (HSPC). CLP, common lymphoid progenitor; MEP, megakaryocyte–erythroid progenitor. Each histogram shows CLL-1 expression (solid red) overlaid with isotype control (gray shade).

bound per cell). No correlation between the expression of CLL-1 and CD33 was observed (Supplementary Fig. S1).

Because CLL-1 expression is limited to the myeloid population of normal human peripheral blood leukocytes, we also wanted to compare its expression level with bone marrow samples from patients with AML. CLL-1 was expressed at a comparable level on normal monocytes as $CD34^+$ AML blasts from patient samples, with lower expression on normal granulocytes. CLL-1 was not detected on the surface of platelets or any lymphocytes, including $CD3^+$ T cells, $CD20^+$ B cells, or $CD56^+$ NK cells. Most importantly, CLL-1 expression was undetectable on $CD34^+/CD38^-$ stem cells from normal donors (Fig. 1B) as has been previously reported (12, 15).

Hematopoietic stem cell and progenitor cells that express surface CLL-1 have restricted hematopoietic potential

As DNA-damaging ADCs can affect normal noncycling cells, we were interested in gaining understanding of the hematopoietic potential of $CLL\text{-}1^+$ cells. To determine when CLL-1 expression begins during hematopoiesis, we used a panel of cell markers to define each differential stage of $CD34^+$ normal hematopoietic stem cell and progenitor cells (HSPC; Fig. 1C). CLL-1 expression was not detected on $CD34^+/CD38^-$ stem cells. In multi-lineage progenitor cell populations, CLL-1 expression was detected on a very small fraction of $CD34^+/CD38^+/CD10^+/CD45RA^+$ common lymphoid progenitor cells, but on at least half the population of $CD34^+/CD38^+/CD10^-/CD45RA^-/CD135^+$ common myeloid progenitor (CMP) cells. Increased CLL-1 expression was detected on the majority of further differentiated $CD34^+/CD38^+/CD10^-/CD45RA^+/CD135^+$ granulocyte–monocyte progenitor (GMP) cells; however, most of the $CD34^+/CD38^+/CD10^-/CD45RA^-/CD135^-$ megakaryocyte–erythroid progenitor cells lost CLL-1 expression. These data suggest that CLL-1 is an early myeloid lineage marker that resides during the differentiation from CMP to GMP cells and could be used to further understand myeloid development.

To further understand the hematopoietic potential of HSPCs expressing CLL-1, we performed CFC assays on $CD34^+$ bone marrow cells. $CD34^+$ cells were first purified from normal human bone marrow aspirate from a total of 4 different healthy donors and then sorted into $CLL\text{-}1^+$ and $CLL\text{-}1^-$ populations. A total of 1,000 cells were plated in each 35-mm dish for scoring different CFU. $CD34^+/CLL\text{-}1^+$ cells only gave rise to colonies

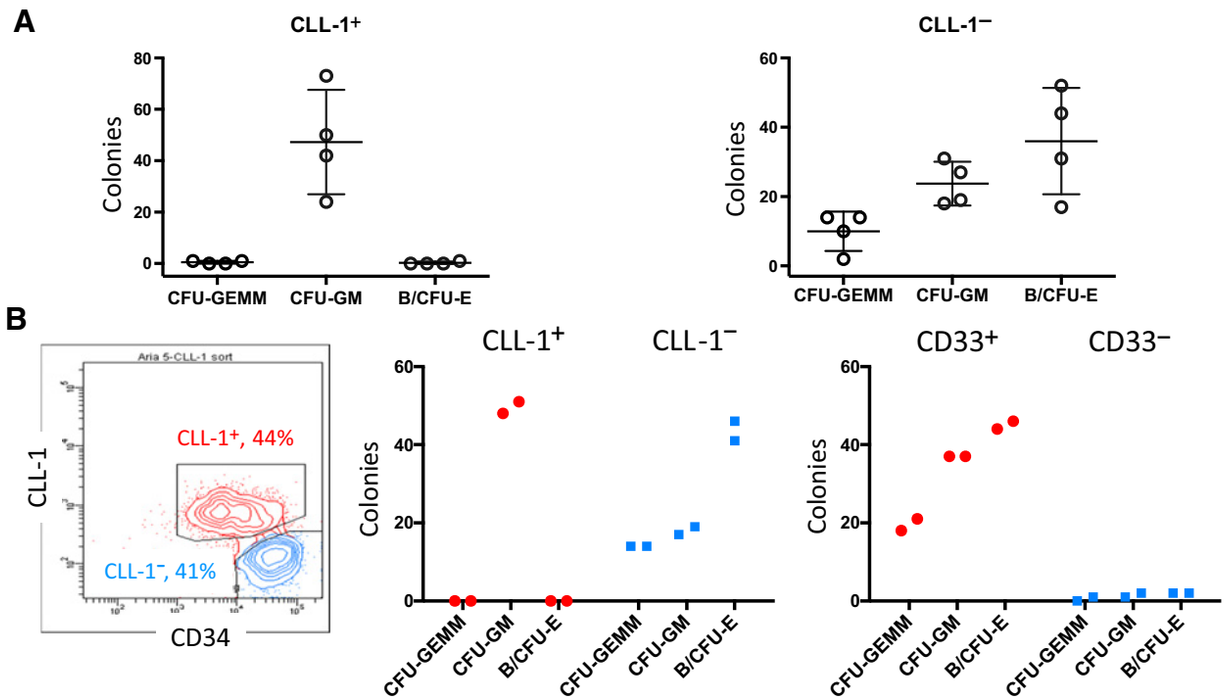

Figure 2.

Colony-forming capacity of CD34$^+$ cells with and without CLL-1 expression. CD34$^+$ cells were purified from normal human bone marrow aspirate and sorted into CLL-1$^+$ and CLL-1$^-$ populations. Colony numbers (mean ± SD) reported were normalized to every 1,000 CD34$^+$ plated cells. **A,** Summary of CFUs from 4 donors. **B,** Representative data from individual donor. Left, sorting strategy and percentage of CLL-1$^+$ and CLL-1$^-$ cells; right, colony-forming capacity of CD34$^+$ cells expressing either CLL-1 or CD33. CFU numbers from duplicate assays were reported.

with myeloid morphology (CFU-GM; Fig. 2A, left) as has been previously reported (12). This strongly suggests that CLL-1 expression begins at the GMP stage and, as described above, is limited to myeloid lineage. More importantly, CD34$^+$/CLL-1$^-$ cells gave rise to colonies with all three groups of morphology, multi-lineage (CFU-GEMM), erythroid (B/CFU-E), and myeloid (Fig. 2A, right), suggesting CD34$^+$/CLL-1$^-$ progenitor cells retain hematopoietic potential. In contrast, the majority of CD34$^+$ HSPCs were CD33$^+$, and CD34$^+$/CD33$^+$ cells gave rise to colonies with all morphologies (Fig. 2B, right), consistent with the broad expression of CD33 on HSCs and all subsequent progenitor cells. Consequently, the few remaining CD34$^+$/CD33$^-$ cells formed only sporadic colonies with any morphology. Collectively, our data provide evidence that, in contrast to CD33, a therapy targeting CLL-1 probably will have less impact on normal hematopoiesis in bone marrow, which in turn may provide better hematopoietic recovery for treated patients.

Anti–CLL-1 antibodies are efficiently internalized

A panel of mAbs against human and cyno CLL-1 were generated by immunizing mice with both recombinant human and cyno CLL-1 extracellular domain (ECD), amino acids 65–265. Five clones reacted strongly by FACS on stable cell lines expressing recombinant human and cyno CLL-1, and on AML tumor cell lines expressing endogenous CLL-1 (9).

Internalization and trafficking to lysosomes upon antibody binding to target is a key component of ADC efficacy (22, 23). To further characterize the potential of CLL-1 as an ADC target, we compared the internalization potential of antibodies with CLL-1 and CD33. AML cell line HL-60 was stained with either DyLight650–labeled anti–CLL-1 antibody or anti-CD33 antibody, and internalization was followed by fluorescence microscopy (Fig. 3A). Both antibodies were rapidly internalized at a similar rate, with intracellular punctate fluorescence from labeled antibodies detected as early as 5 minutes. CLL-1 antibodies were also found to be efficiently targeted to the lysosome (Supplementary Fig. S2)

Generation of an anti–CLL-1 ADC

A lead anti–CLL-1 antibody was selected, humanized, and engineered for improved chemical stability based on its antigen-binding affinity, *in vitro* and *in vivo* efficacy, and drug metabolism and pharmacokinetic properties (manuscript in preparation). The binding epitope of this optimized antibody, hu6E7.N54A, was determined by hydroxyl radical footprinting on antigen (CLL-1 ECD) and antigen–mAb complexes. The overall sequence coverage obtained using trypsin mapping was 90.05%. The PR for most of the peptides was approximately equal to 1, indicating minimal change in solvent accessibility for the corresponding regions (Supplementary Table S1). Only a single peptide that corresponds to amino acids 142–158 of human CLL-1 exhibited a PR value of 3.1 (Fig. 3B), suggesting the antigen–antibody complex confers significant protection for this specific region. These data suggest that "DSCYFLSDDVQTWQESK" (aa142–158), located within the C-type lectin-like domain

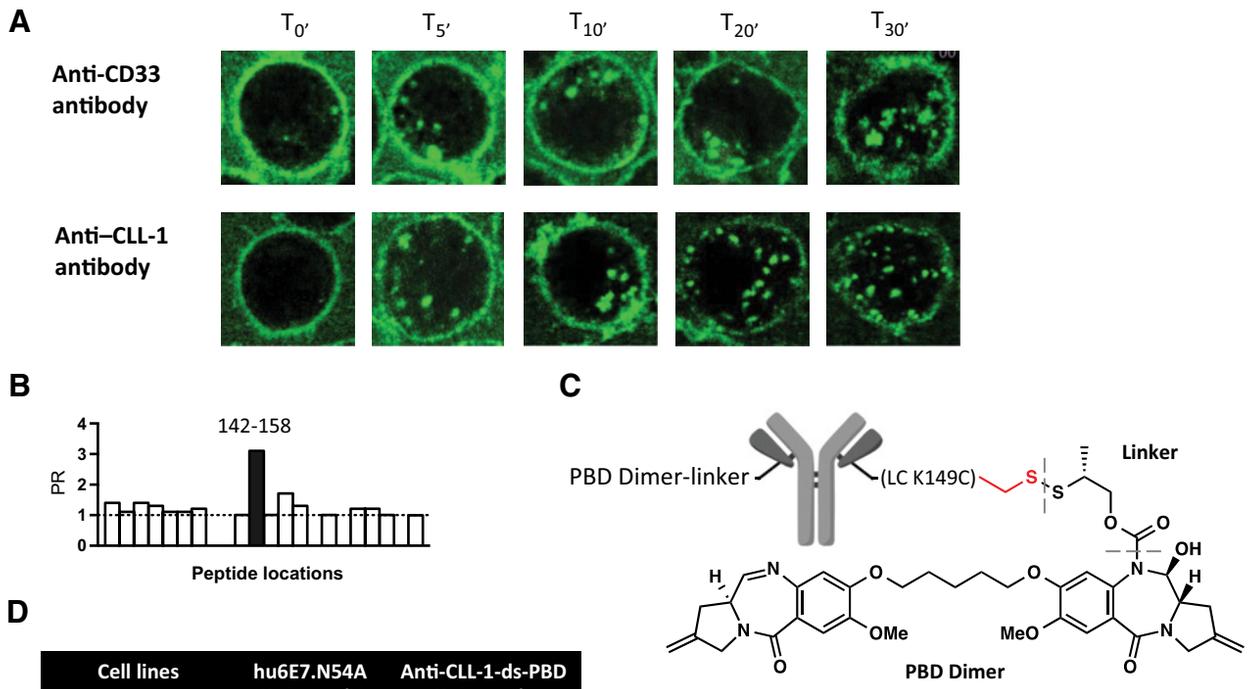

D

Cell lines	hu6E7.N54A K_D (nmol/L)	Anti-CLL-1-ds-PBD K_D (nmol/L)
HL-60	1.10 ± 0.11	1.24 ± 0.11
293AD/cynoCLL-1	0.79 ± 0.09	0.70 ± 0.05

Figure 3.

Property of anti–CLL-1 antibody and anti–CLL-1-ds-PBD. **A,** Rapid internalization of anti–CLL-1 antibodies on HL-60 cells. AML cell line HL-60 was stained with either DyLight-488–labeled anti-CD33 antibody or anti–CLL-1 antibody. Images were taken at different time points after adding labeled antibodies, as indicated. **B,** PR of different peptides from hydroxyl radical footprinting (HRF) assay. Dotted line represents a PR of 1, which indicates a minimal protection. Region 142–158 (solid black column) showed a PR value of 3.1, suggesting the antigen–antibody complex confers significant protection for this specific region. **C,** Structure of anti–CLL-1-ds-PBD. Only one PBD dimer attached to a cysteine engineered into the light chain of antibody is shown for clarity. **D,** Binding affinity of anti–CLL-1 antibody (hu6E7.N54A) and anti–CLL-1-ds-PBD to human and cyno CLL-1 antigen.

(CTLD) of CLL-1 protein, is most likely the epitope of anti-human CLL-1 antibody, hu6E7.N54A.

We chose a novel and more stable linker-drug for our anti–CLL-1 ADC, a pyrrolo [2,1-c][1,4] benzodiazepine dimer attached to an engineered cysteine at K149C site of the human IgG light chain via a self-immolative disulfide linker (18, 19). PBDs are highly potent natural product antitumor agents that bind covalently in the minor groove of DNA and form interstrand and intrastrand cross-linked adducts as well as monoadducts (24–26). We will refer to this THIOMAB ADC as anti–CLL-1-ds-PBD (Fig. 3C). This ADC retained the same high-binding affinity to both human and cyno CLL-1 with a KD of approximately 1 nmol/L as the parental antibody alone (Fig. 3D).

Efficacy studies of anti–CLL-1-ds-PBD

The antitumor activity of anti–CLL-1-ds-PBD was first assessed in a panel of CLL-1$^+$ AML cell lines and AML patient samples (Table 1). Anti–CLL-1-ds-PBD was found to be highly

Table 1. *In vitro* antitumor activity of anti–CLL-1-ds-PBD

Samples	CLL-1 expression (normalized gMFI)	Cytogenetic risk	Anti–CLL-1-ds-PBD IC_{50} (ng/mL)	Nonbinding control ADC IC_{50} (ng/mL)
Patient #1	1,949	Favorable	34	86
Patient #2	974	Adverse	39	133
Patient #3	1,671	Adverse	40	208
Patient #4	287	Intermediate	186	189
Patient #5	1,109	Adverse	118	175
HL-60	2,145 ± 145	n/a	10 ± 2	109 ± 7
EOL-1	263 ± 27	n/a	8 ± 2	27 ± 5
THP-1	394 ± 38	n/a	81 ± 9	58 ± 8

NOTE: CLL-1 expression of AML blast from patients or AML cell lines was measured at the start of the treatment; gMFI (geomean fluorescence intensity) value was normalized to Rainbow Fluorescent Particles (BD Biosciences) to enable comparison among samples. IC_{50} is defined as the concentration of ADC needed to yield a 50% reduction in viability compared with vehicle-treated cells. AML cell line gMFI and IC_{50} value are mean ± SD of three independent experiments.

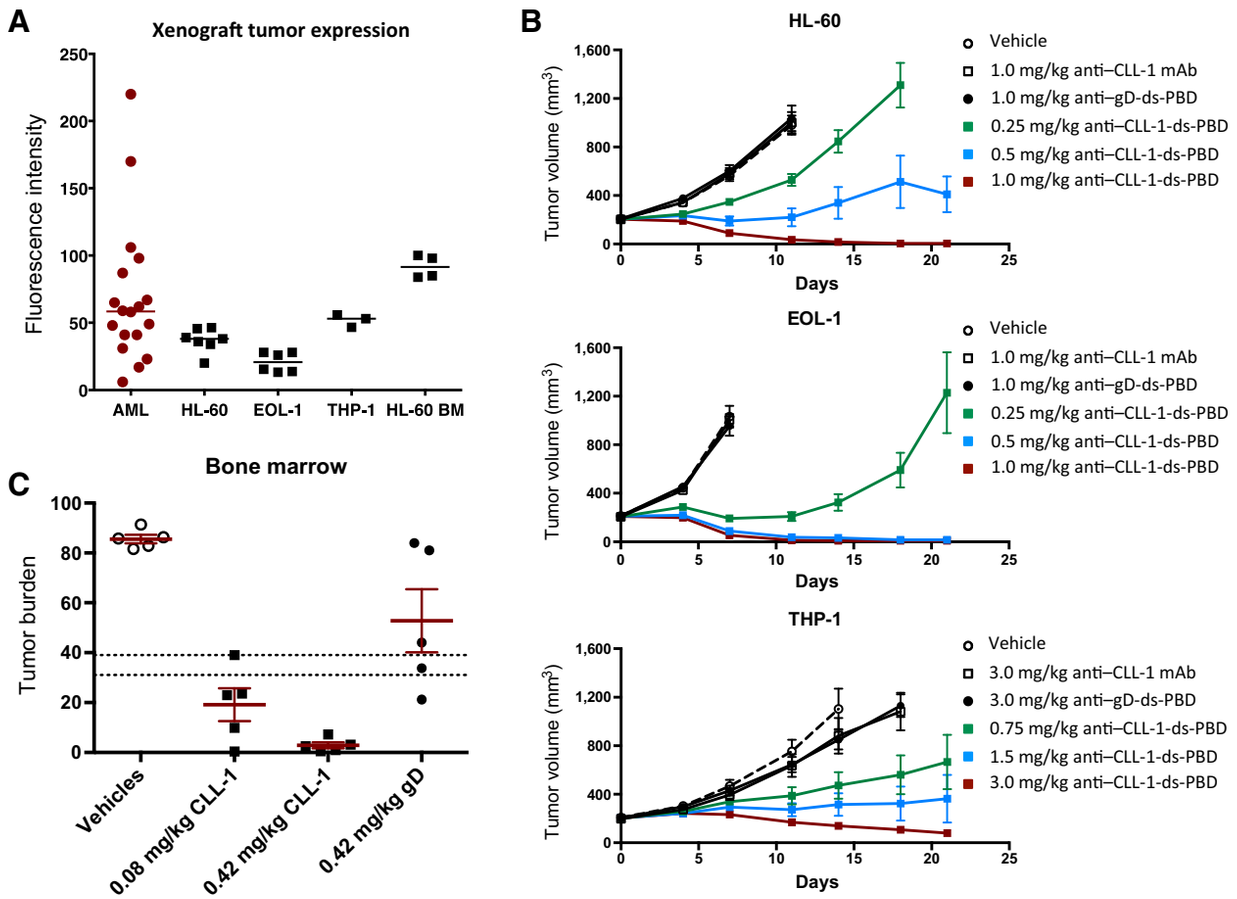

Figure 4.

In vivo efficacy of anti–CLL-1-ds-PBD in xenograft tumor models. **A,** Expression level of CLL-1 in xenograft tumors. Median value of expression was indicated by a solid line. BM, bone marrow. **B,** Subcutaneous models of HL-60, EOL-1, and THP-1. Group mean (±SEM) tumor volumes over the duration of the study are shown for animals (n = 8/group) administered with a single intravenous dose of vehicle, anti–gD-ds-PBD (nontargeting control), anti–CLL-1 antibody or anti–CLL-1-ds-PBD at the dose level indicated. **C,** Disseminated model of HL-60. Individual (circle or square) and group mean (±SEM; red solid line) tumor burdens (n = 5/group) at 2 weeks after vehicle or ADC dose are shown. Range of baseline tumor burden at the time of dosing was indicated by black dotted lines.

active against primary AML patient samples with the IC_{50} range from 34 to 186 ng/mL, similar to that observed in AML cell lines (10–81 ng/mL). No obvious correlation between ADC activity and CLL-1 expression or cytogenetic risk was observed. High background cytotoxicity from nonbinding control ADC was observed in patient #4 and THP-1 cells; nevertheless, the same control ADC had minimal effect on tumor growth in THP-1 xenograft model as described below.

To further understand the therapeutic potential of anti–CLL-1-ds-PBD, we assessed the antitumor activity in various xenograft tumor models established in immunocompromised C.B-17 Fox Chase SCID mice from the same three human AML cell lines used above. These models expressed CLL-1 at levels within the range observed in patients with AML as determined by FACS (Fig. 4A) and harbor cytogenetic features of patients with AML that typically have poor prognosis. The unconjugated anti–CLL-1 antibody and a nonbinding control conjugate (anti–gD-ds-PBD) had no effect on tumor growth. The lack of activity of the unconjugated antibody is expected, as the anti–CLL-1 antibody is highly internalized and thus not available for Fc-mediated killing. Also, the nonbinding control showed minimal efficacy, suggesting a high degree of *in vivo* specificity. In contrast, anti–CLL-1-ds-PBD demonstrated clear dose-dependent inhibition of tumor growth in all three models (Fig. 4B). The EOL-1 and HL-60 xenograft tumors were completely ablated by a single dose of 1 mg/kg anti–CLL-1-ds-PBD. The THP-1 xenograft model, known to be less responsive to cytarabine (27), required a higher dose (3 mg/kg) of anti–CLL-1-ds-PBD in order to regress tumors. All doses were tolerated with minimal bodyweight loss and no signs of moribundity (data not shown).

To assess the antitumor activity of anti–CLL-1-ds-PBD in an AML model that is more disease relevant, we developed a disseminated HL-60 xenograft tumor model (Fig. 4C). Animals were implanted with tumor cells intravenously through tail vein and tumors were allowed to establish in bone marrow before being dosed with ADCs. Tumor burden was defined as the percentage of human HL-60 cells relative to total mouse bone marrow leukocytes. Anti–CLL-1-ds-PBD was effective in inhibiting the tumor growth in bone marrow. A single dose of

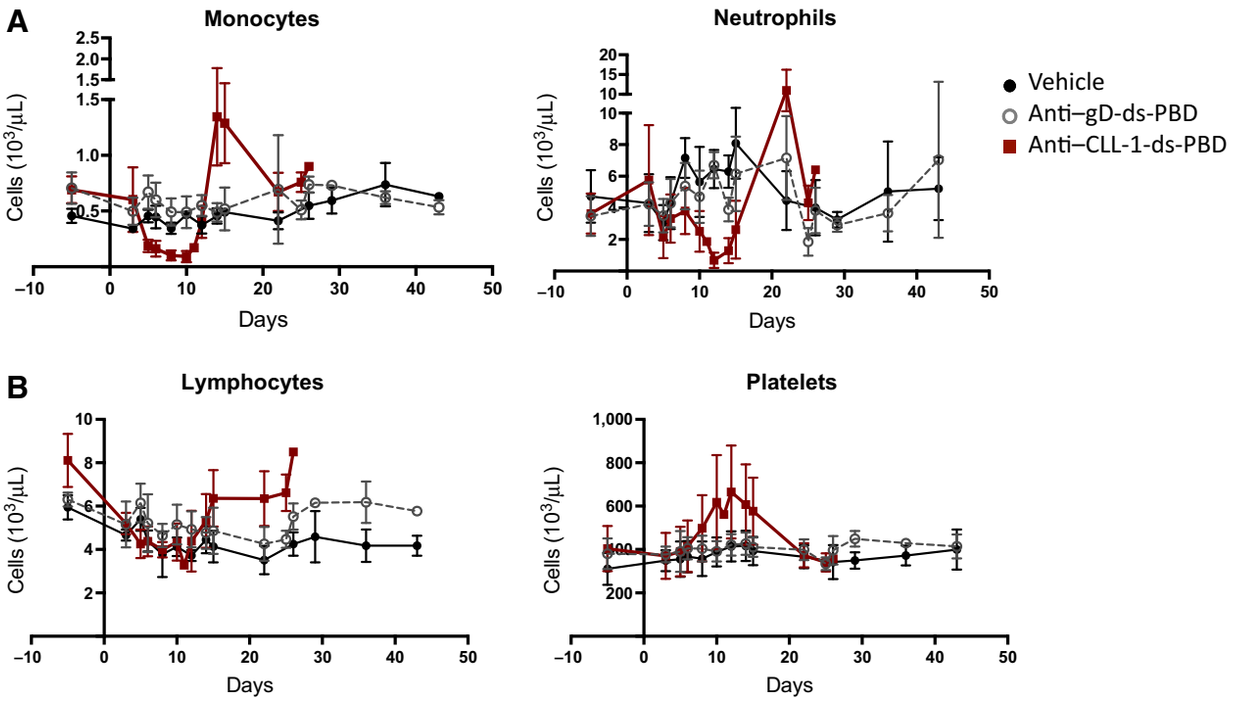

Figure 5.

Target-dependent depletion of myeloid cells followed by recovery in cynomolgus monkeys. 0.1 mg/kg single dose of anti–CLL-1-ds-PBD is shown, and similar result was observed for 0.2 mg/kg dose level. Anti–gD-ds-PBD was dosed at 0.4 mg/kg. Predose baseline cell counts were determined as average through several days, and plotted as day −5. **A,** On-target populations (monocytes and neutrophils) were depleted by days 8 to 12 with recovery by day 14/15 for monocytes and day 22 for neutrophils. **B,** Nontargeted populations (lymphocytes and platelets) were not affected.

0.08 mg/kg reduced the mean (±SEM) tumor burden to 19.15% ± 6.59% of total leukocytes, compared with vehicle with mean tumor burden of 85.58% ± 1.68%. A 0.42 mg/kg dose of anti–CLL-1-ds-PBD further reduced the tumor burden to 2.84% ± 1.19%, and averted the mouse bodyweight loss and signs of moribundity associated with tumor burden (data not shown).

Target-dependent toxicity of anti–CLL-1-ds-PBD

We evaluated the target-dependent tolerability and toxicity of anti–CLL-1-ds-PBD in cynomolgus monkeys as they were the most suitable species for safety studies. Cynomolgus monkeys express CLL-1 on normal monocytes and granulocytes, albeit at lower levels than humans; and, unlike humans, cynomolgus monkeys do express very low level of CLL-1 on $CD34^+CD38^-$ stem cells (9).

Monkeys were administered a single intravenous dose of 0.1 and 0.2 mg/kg of anti–CLL-1-ds-PBD (n = 2–3/sex/group). These doses were tolerated, and all animals were euthanized on day 25 or 26 after recovery of granulocytes was observed. Clinical observations were limited to swelling and/or darkening of the skin at the injection site (day 1), hunched appearance, and decreased activity (days 6–7). Hematology findings at both dose levels included moderate to marked decreases in granulocytes (neutrophils, eosinophils, basophils) and monocytes (Fig. 5A) that reached a nadir at days 8 to 12 and rebounded/recovered by day 14/15 (monocytes and basophils) or day 22 (neutrophils). Cells known to lack CLL-1 expression, including lymphocytes and platelets, were not affected (Fig. 5B). Other changes in hematology parameters, generally beginning on day 3 or 5, included a moderate transient reduction in reticulocytes associated with minimally decreased red blood cell mass in individual animals. There were no changes in clinical chemistry or coagulation parameters. Microscopic findings were limited to bone marrow hypercellularity with increases in phagocytosis of cellular debris, extramedullary hematopoiesis in the spleen and lymph node, and increased pigmentation and epidermal thickening of the skin of the injection site.

As human patients are able to access extensive supportive care to tolerate cytopenias, particularly neutropenia and neutropenia-related infections, we also wanted to understand target-independent toxicities. Cynomolgus monkeys were administrated with 0.4 and 1.0 mg/kg anti–gD-ds-PBD ADC, a non-target-binding reagent. Clinical pathology parameters were generally minor and without microscopic correlates and were limited to mildly decreased reticulocytes, minimally decreased red blood cell mass in females at 1.0 mg/kg only, decreased eosinophils, mildly prolonged activated partial thromboplastin time in individual animals, and mildly decreased phosphorus in males at 0.4 mg/kg only. Importantly, no decreases in neutrophils, lymphocytes, or platelets were observed in animals administered anti–gD-ds-PBD ADC.

Discussion

Several lines of evidence suggest that intensification of chemotherapy through the use of ADCs has the potential to increase OS

in patients with AML. Gemtuzumab ozogamicin is the first approved ADC by FDA and currently the only ADC approved for the treatment of AML. In 2000, gemtuzumab ozogamicin was given accelerated approval by the FDA as monotherapy for older unfit patients with AML that experienced initial relapse. However, it was withdrawn from the market in 2010 after a confirmatory trial failed to demonstrate OS benefit and an unexpectedly increased rate of earlier mortality. More recently, gemtuzumab ozogamicin was reapproved by FDA when subsequent trials of gemtuzumab ozogamicin in newly diagnosed patients with AML demonstrated improved efficacy and reduced toxicity using a modified fractionated schedule at a lower dose than the one described for the initial approval. Despite the improved risk-benefit of gemtuzumab ozogamicin with the modified dose and schedule, patients still experienced persistent thrombocytopenia and continued to have a higher risk of veno-occlusive disease (28, 29). Other attempts to develop ADCs for AML have also yielded important clues about factors that limit their effectiveness. AVE9633 (immunogen) is an anti-CD33–maytansinoid that was safe but ineffective at target-saturating dose levels. This lack of activity was probably due to the use of a maytansinoid, a tubulin inhibitor, as the cytotoxic payload, which has the same mechanism of action as vincristine, a drug that has been shown to be ineffective in AML (30). A more promising example is vadastuximab talirine, an anti-CD33 antibody with engineered cysteines, conjugated via a protease-cleavable linker to a highly potent PBD dimer (7). In phase I studies, vadastuximab talirine was found to be effective, 5 (out of 18) patients achieved CR at the recommended 40 μg/kg dose level (10). However, the median time to full count recovery in patients across all the dose levels was 6.4 weeks for neutrophils and 10.6 weeks for platelets. This prolonged neutrophil and platelet recovery limited the amount of drug that could be administered and its ability to be combined with other myelotoxic regimens (31).

The clinical experiences of gemtuzumab ozogamicin, vadastuximab talirine, and other ADC attempts highlight the challenges of developing an ADC for the treatment of AML and support the need of further improvements of this promising approach. The success of a new ADC therapy hinges on the delicate balance between potency and safety; described herein are several approaches we employed to optimize this balance.

An important consideration for an ADC approach for AML is likely to be target selection. All of the aforementioned ADCs in clinical development in AML target CD33 (32–34). Although CD33 is a compelling target based on its broad expression on AML blasts, its expression on normal HSCs indicates that prolonged cytopenias among multiple hematopoietic lineages may limit the clinical benefit of CD33-targeting agents (35). Clinical trials for vadastuximab talirine have recently been discontinued because of increased infectious death in the experiment arm, probably due to prolonged neutrophil recovery (http://www.seattlegenetics.com). CD123 is another ADC target for AML that is currently in clinical trials (SGN-CD123A, NCT02848248). However, its expression on normal HSCs raises the similar concerns of on-target off-tumor toxicity as for CD33 (9, 36, 37). Therefore, we have chosen an emerging LSC marker CLL-1 as our target. Here, we show that CLL-1 shares similar prevalence and trafficking properties that make CD33 an excellent ADC target for AML, but lacks the HSC expression that may be hampering current CD33 and CD123 targeted ADCs. The HSPC expression profile and colony formation assays described in this report further suggest that depletion of $CD34^+/CLL\text{-}1^+$ progenitor cells should not impair patients' normal hematopoietic potential or induce persistent thrombocytopenia, which are major concerns for CD33-based ADCs. This belief is also supported by our previous studies using a CLL-1 T cell–dependent bispecific antibody (TDB) that was shown to spare the hematopoietic potential of human bone marrow cells, upon exposure to a CLL-1 TDB *in vitro* (9). Because of this more restricted expression pattern of CLL-1, targeting this molecule, although still will cause depletion of myeloid cells, could provide a more favorable safety profile through quicker recovery from cytopenias.

We selected PBD dimer, which is a clinically proven DNA-damaging agent and similar to that used in vadastuximab talirine (31, 38), as our cytotoxic payload. However, rather than a protease-cleavable linker, we have developed a novel self-immolative disulfide linker and conjugated to an engineered cysteine residue at K149C site on the human IgG light chain. This combination of disulfide linker and antibody site has been shown to provide good stability and release properties for the conjugated PBD dimer, exhibits equivalent efficacy in xenograft studies, and is better tolerated with an MTD four times higher than the peptide-linked PBD ADC in preclinical rat models (19).

Target-independent side effects from payloads have usually limited the MTD in previous ADC therapies. Vascular leak has been reported as a dose-limiting toxicity (DLT) in clinical trials with PBD dimer both as a free drug and as an ADC (26, 39). However, in cynomolgus monkeys, both 0.1 and 0.2 mg/kg of anti–CLL-1-ds-PBD induced target cell depletion, but no target-independent side effects were observed. More importantly, no edema or hemorrhage related to vascular leak was observed. A nontargeting but otherwise identical ADC was well tolerated at twice the dose (0.4 mg/kg), with no observed decreases in neutrophils, lymphocytes, or platelets. The DLT of anti–CLL-1-ds-PBD ADC in cynomolgus monkeys is defined as the targeted depletion of neutrophils, but not lymphocytes or platelets and is predicted to be the case in humans as well. However, neutropenia is an expected and common side effect of AML treatment; there is extensive clinical experience in its management and mitigation, which is not typically available in preclinical safety studies. Furthermore, full recovery of neutrophils was observed in cynomolgus monkeys at day 22. In summary, our anti–CLL-1-ds-PBD described here is highly effective at depleting tumors cells in AML xenograft models and lacks target-independent toxicities at doses that depleted target myeloid cells in cynomolgus monkeys. Our data therefore suggest that it has the potential to become an effective treatment for AML in humans and resolve some limitations of the current generation of ADCs.

Disclosure of Potential Conflicts of Interest

A.G. Polson, B. Zheng, S.R. Leong, R. Vij, J. Sadowsky, and Y. Chu hold ownership interest (including patents) in Roche/Genentech. No potential conflicts of interest were disclosed by the other authors.

Authors' Contributions

Conception and design: B. Zheng, S.-F. Yu, C. Chalouni, J. Sadowsky, T. Pillow, M.M. Schutten, J. Flygare, A.G. Polson

Development of methodology: B. Zheng, S.-F. Yu, S.R. Leong, C. Chiu, J. Sadowsky
Acquisition of data (provided animals, acquired and managed patients, provided facilities, etc.): B. Zheng, S.-F. Yu, G. Del Rosario, S.R. Leong, R. Vij, C. Chiu, W.-C. Liang, Y. Wu, C. Chalouni, J. Sadowsky, K.A. Poon
Analysis and interpretation of data (e.g., statistical analysis, biostatistics, computational analysis): B. Zheng, S.-F. Yu, G. Del Rosario, S.R. Leong, R. Vij, W.-C. Liang, Y. Wu, K.A. Poon, M.M. Schutten, J. Flygare
Writing, review, and/or revision of the manuscript: B. Zheng, S.-F. Yu, S.R. Leong, G.Y. Lee, C. Chiu, V. Clark, W. Chu, T. Pillow, M.M. Schutten, J. Flygare, A.G. Polson
Administrative, technical, or material support (i.e., reporting or organizing data, constructing databases): V. Clark, M.M. Schutten, J. Flygare, A.G. Polson
Study supervision: S.-F. Yu, Y. Wu, C. Chalouni, V. Clark, A. Hendricks, K.A. Poon, J. Flygare
Other (project management): G.Y. Lee
Other (advised on experimental design for the study of the internalization of anti–CCL-1 ADC, performed microscopy imaging, and wrote the conclusions of this part of the study): C. Chalouni

Acknowledgments

The authors would like to thank Elizabeth Luis for conducting equilibrium binding assay.

The costs of publication of this article were defrayed in part by the payment of page charges. This article must therefore be hereby marked *advertisement* in accordance with 18 U.S.C. Section 1734 solely to indicate this fact.

Received January 30, 2018; revised May 7, 2018; accepted June 25, 2018; published first June 29, 2018.

References

1. Estey EH. Therapeutic options for acute myelogenous leukemia. Cancer 2001;92:1059–73.
2. Appelbaum FR, Gundacker H, Head DR, Slovak ML, Willman CL, Godwin JE, et al. Age and acute myeloid leukemia. Blood 2006;107: 3481–5.
3. Stone RM, Mandrekar SJ, Sanford BL, Laumann K, Geyer S, Bloomfield CD, et al. Midostaurin plus Chemotherapy for Acute Myeloid Leukemia with a FLT3 Mutation. N Engl J Med 2017;377:454–64.
4. Stein EM, DiNardo CD, Pollyea DA, Fathi AT, Roboz GJ, Altman JK, et al. Enasidenib in mutant IDH2 relapsed or refractory acute myeloid leukemia. Blood 2017;130:722–31.
5. Fernandez HF, Sun Z, Yao X, Litzow MR, Luger SM, Paietta EM, et al. Anthracycline dose intensification in acute myeloid leukemia. N Engl J Med 2009;361:1249–59.
6. Brunetti C, Anelli L, Zagaria A, Specchia G, Albano F. CPX-351 in acute myeloid leukemia: can a new formulation maximize the efficacy of old compounds? Expert Rev Hematol 2017;10:853–62.
7. Kung Sutherland MS, Walter RB, Jeffrey SC, Burke PJ, Yu C, Kostner H, et al. SGN-CD33A: a novel CD33-targeting antibody-drug conjugate using a pyrrolobenzodiazepine dimer is active in models of drug-resistant AML. Blood 2013;122:1455–63.
8. Sutherland MSK, Yu C, O'Day C, Alley S, Anderson M, Emmerton K, et al. SGN-CD33A in combination with hypomethylating agents is highly efficacious in preclinical models of AML. Blood 2015;126:3785–5.
9. Leong SR, Sukumaran S, Hristopoulos M, Totpal K, Stainton S, Lu E, et al. An anti-CD3/anti-CLL-1 bispecific antibody for the treatment of acute myeloid leukemia. Blood 2017;129:609–18.
10. Stein EM, Walter RB, Erba HP, Fathi AT, Advani AS, Lancet JE, et al. A phase 1 trial of vadastuximab talirine as monotherapy in patients with CD33 positive acute myeloid leukemia (AML). Blood 2018; 131:387–96.
11. Bakker ABH, van den Oudenrijn S, Bakker AQ, Feller N, van Meijer M, Bia JA, et al. C-type lectin-like molecule-1: a novel myeloid cell surface marker associated with acute myeloid leukemia. Cancer Res 2004; 64:8443–50.
12. van Rhenen A, van Dongen GAMS, Kelder A, Rombouts EJ, Feller N, Moshaver B, et al. The novel AML stem cell associated antigen CLL-1 aids in discrimination between normal and leukemic stem cells. Blood 2007;110:2659–66.
13. Marshall ASJ, Willment JA, Lin H-H, Williams DL, Gordon S, Brown GD. Identification and characterization of a novel human myeloid inhibitory C-type lectin-like receptor (MICL) that is predominantly expressed on granulocytes and monocytes. J Biol Chem 2004;279: 14792–802.
14. Marshall ASJ, Willment JA, Pyz E, Dennehy KM, Reid DM, Dri P, et al. Human MICL (CLEC12A) is differentially glycosylated and is down-regulated following cellular activation. Eur J Immunol 2006;36:2159–69.
15. Larsen HØ, Roug AS, Just T, Brown GD, Hokland P. Expression of the hMICL in acute myeloid leukemia-a highly reliable disease marker at diagnosis and during follow-up. Cytometry B Clin Cytom 2012;82:3–8.
16. Terwijn M, Zeijlemaker W, Kelder A, Rutten AP, Snel AN, Scholten WJ, et al. Leukemic stem cell frequency: a strong biomarker for clinical outcome in acute myeloid leukemia. PLoS One 2014;9:e107587.
17. Darwish NHE, Sudha T, Godugu K, Elbaz O, Abdelghaffar HA, Hassan EEA, et al. Acute myeloid leukemia stem cell markers in prognosis and targeted therapy: potential impact of BMI-1, TIM-3 and CLL-1. Oncotarget 2016;7:57811–20.
18. Pillow TH, Sadowsky JD, Zhang D, Yu S-F, Del Rosario G, Xu K, et al. Decoupling stability and release in disulfide bonds with antibody-small molecule conjugates. Chem Sci 2016;8:366–70.
19. Pillow TH, Schutten M, Yu S-F, Ohri R, Sadowsky J, Poon KA, et al. Modulating therapeutic activity and toxicity of pyrrolobenzodiazepine antibody-drug conjugates with self-immolative disulfide linkers. Mol Cancer Ther 2017;16:871–78.
20. Takamoto K, Chance MR. Radiolytic protein footprinting with mass spectrometry to probe the structure of macromolecular complexes. Annu Rev Biophys Biomol Struct 2006;35:251–76.
21. Yu S-F, Zheng B, Go MA, Lau J, Spencer S, Raab H, et al. A novel anti-CD22 anthracycline-based antibody-drug conjugate (ADC) that overcomes resistance to auristatin based ADCs. Clin Cancer Res 2015;21: 3298–306.
22. Bakhtiar R. Antibody drug conjugates. Biotechnol Lett 2016;38:1655–64.
23. Thomas A, Teicher BA, Hassan R. Antibody-drug conjugates for cancer therapy. Lancet Oncol 2016;17:e254–62.
24. Hartley JA. The development of pyrrolobenzodiazepines as antitumour agents. Expert Opin Investig Drugs 2011;20:733–44.
25. Hartley JA, Hamaguchi A, Suggitt M, Gregson SJ, Thurston DE, Howard PW. DNA interstrand cross-linking and in vivo antitumor activity of the extended pyrrolo[2,1-c][1,4]benzodiazepine dimer SG2057. Invest New Drugs 2012;30:950–8.
26. Mantaj J, Jackson PJM, Rahman KM, Thurston DE. From anthramycin to pyrrolobenzodiazepine (PBD)-containing antibody-drug conjugates (ADCs). Angew Chem Int Ed Engl 2017;56:462–88.
27. Yamauchi T. Characterization of cytarabine-resistant leukemic cell lines established from five different blood cell lineages using gene expression and proteomic analyses. Int J Oncol 2011;38:911–9.
28. Laing AA, Harrison CJ, Gibson BES, Keeshan K. Unlocking the potential of anti-CD33 therapy in adult and childhood acute myeloid leukemia. Exp Hematol 2017;54:40–50.
29. Godwin CD, Gale RP, Walter RB. Gemtuzumab ozogamicin in acute myeloid leukemia. Leukemia 2017;31:1855–68.
30. Lapusan S, Vidriales MB, Thomas X, de Botton S, Vekhoff A, Tang R, et al. Phase I studies of AVE9633, an anti-CD33 antibody-maytansinoid conjugate, in adult patients with relapsed/refractory acute myeloid leukemia. Invest New Drugs 2012;30:1121–31.
31. Fathi AT, Erba HP, Lancet JE, Stein EM, Ravandi F, Faderl S, et al. Vadastuximab Talirine Plus Hypomethylating Agents: A Well-Tolerated Regimen with High Remission Rate in Frontline Older Patients with Acute Myeloid Leukemia (AML). Blood 2016;128:591.
32. Garfin PM, Feldman EJ. Antibody-based treatment of acute myeloid leukemia. Curr Hematol Malig Rep 2016;11:545–52.

33. Bose P, Vachhani P, Cortes JE. Treatment of relapsed/refractory acute myeloid leukemia. Curr Treat Options Oncol 2017;18:17.
34. Lichtenegger FS, Krupka C, Haubner S, Köhnke T, Subklewe M. Recent developments in immunotherapy of acute myeloid leukemia. J Hematol Oncol 2017;10:142.
35. Walter RB, Appelbaum FR, Estey EH, Bernstein ID. Acute myeloid leukemia stem cells and CD33-targeted immunotherapy. Blood 2012;119:6198–208.
36. Taussig DC, Pearce DJ, Simpson C, Rohatiner AZ, Lister TA, Kelly G, et al. Hematopoietic stem cells express multiple myeloid markers: implications for the origin and targeted therapy of acute myeloid leukemia. Blood 2005;106:4086–92.
37. Testa U, Pelosi E, Frankel A. CD 123 is a membrane biomarker and a therapeutic target in hematologic malignancies. Biomark Res 2014; 2:4.
38. Hochhauser D, Meyer T, Spanswick VJ, Wu J, Clingen PH, Loadman P, et al. Phase I study of sequence-selective minor groove DNA binding agent SJG-136 in patients with advanced solid tumors. Clin Cancer Res 2009;15: 2140–7.
39. Puzanov I, Lee W, Chen AP, Calcutt MW, Hachey DL, Vermeulen WL, et al. Phase I pharmacokinetic and pharmacodynamic study of SJG-136, a novel DNA sequence selective minor groove cross-linking agent, in advanced solid tumors. Clin Cancer Res 2011;17: 3794–802.